

Ocular monochromatic aberration statistics in a large emmetropic population

S. Plainis* and I.G. Pallikaris

*Institute of Vision and Optics (IVO), University of Crete,
Heraklion, Greece*

(Received 16 January 2007; final version received 3 April 2007)

The primary objective of this study was to explore the statistics of ocular higher-order aberrations in a nearly emmetropic population. The wavefront aberration of 393 eyes of 218 subjects was obtained under natural conditions using the WaveLight WaveFront Analyser. The spherical equivalent of eyes ranged between +0.75 and -1.25 D, with the astigmatism being less than 0.75 D. Mean age was 33.0 ± 4.8 years. Analysis was performed for a 6 mm pupil. A significant dispersion in all Zernike coefficients was found. Population average values of Zernike coefficients were almost zero, with the exemption of primary spherical ($c_4^0, 0.037 \mu\text{m}$) and oblique trefoil ($c_3^{-3}, -0.062$) aberrations. Mean higher-order RMS error was $0.26 \mu\text{m}$, corresponding to an equivalent defocus of 0.20 D. An increase in higher-order RMS with age (at pre-presbyopic range) was found, which was accompanied by changes in coma-like aberrations, while spherical aberration remained unchanged. Emmetropic eyes appear to have on average lower individual and combined higher-order aberrations than previously reported values on myopic eyes. Although aberration levels at fixed pupil diameter increase with age, their effect on retinal image quality is possibly cancelled out by senile miosis.

Keywords: ocular aberrations; emmetropes; ageing; spherical aberration; bilateral symmetry

1. Introduction

Although the concept of ocular aberration was introduced in early 1950s to 1960s [1–3], it was not until the emergence of sophisticated diagnostic instrumentation for its evaluation that it attracted the attention of ophthalmic practitioners and clinical researchers. Since then, there has been a considerable research concerning the statistics of ocular higher order aberrations in large populations [4–8], their impact on retinal image quality [7, 9, 10] and spatial visual performance [11, 12]. Furthermore, a number of studies have reported changes in the magnitude of higher order aberrations (HOA) with age [4, 13–15], upon accommodation [11, 16–18] and following refractive surgery [19, 24]. More recently, there have been suggestions of the prospective use of wavefront aberrometers as a better alternative to the

*Corresponding author. Email: plainis@med.uoc.gr

automated sphero-cylindrical refractors, since the optimal refractive correction can be deduced from the Zernike terms or the use of a number of image metrics [25–27].

In normal eyes, the impact of higher order aberrations to retinal blur is far outweighed by defocus and astigmatism. When sphero-cylindrical refractive error is spectacle- or contact lens-corrected, retinal image quality is limited by diffraction, scatter and the magnitude of higher order aberrations. Diffraction of the eye's pupil has a profound effect on retinal image only when the pupil is smaller than 2.0 mm [28, 29], becoming less important at pupil sizes encountered at daytime conditions [30]. On the other hand, scatter is generally a minor source of blur, degrading vision only in older and/or pathological eyes [31–34]. As a consequence, in the absence of any refractive error, higher order aberrations, together with longitudinal chromatic aberration [35], form the main optical limitation on foveal vision.

There have been recent large-scale studies on the prevalence of higher order aberrations in healthy eyes. However, when comparing results from these studies there are some confounding factors, such as the age range and the refractive status of the sample population. For example, Porter et al. [6], Castejon-Mochon et al. [5] and Carkeet et al. [36] included uncorrected ametropic eyes with high refractive error (up to -12 D), whereas other studies measured wave aberrations of spectacle-corrected subjects drawn from a student population [7, 37] or a refractive surgery clinic [8].

Since there are suggestions that the magnitude of higher-order aberrations increases with myopic refractive error [36, 38, 39], their effect on the retinal image quality might have been overestimated (see [7]). Moreover, there is evidence that, due to pupil magnification, the magnitude of aberrations is over/under-estimated when the eyes are corrected with spectacle lenses, depending upon the sign and vertex distance of spectacle correction. For example, a negative spectacle correction minifies the entrance pupil of the eye leading to increased amounts (overestimation) of spherical aberration [37, 40].

Therefore, in order to make safe conclusions regarding the prevalence and the role of aberrations in the absence of any sphero-cylindrical refractive error, and their involvement in myopisation through image degradation at the fovea, it is necessary to determine aberration data from emmetropic eyes. The objective of this study was to use a commercially-available wavefront sensor, based on Tscherning optics, to explore distribution statistics of monochromatic aberrations in a nearly-emmetropic population.

2. Methods

2.1 Subjects

393 eyes of 218 subjects were tested. All subjects were professional referees of the Greek Football Federation with normal vision (by the rules, uncorrected monocular decimal visual acuity should be ≥ 0.8). Mean age was 33.1 ± 4.8 years (range: 21–43). In total, 274 referees were examined, but eyes with spherical equivalent >1.25 D or cylindrical error >0.75 D were excluded from further analysis. The spherical equivalent of the subjects, as measured by an automated auto-refractometer (Canon RK-F1, Tokyo, Japan), was -0.25 ± 0.47 (range: -1.25 to 1.13 D). No spectacle – or contact – lens correction was used (it should be noted that football referees in Greece are not allowed to wear any

optical correction during play). All subjects were free of ocular or corneal disease and had normal binocular and colour vision. Uncorrected logMAR visual acuity (VA) ranged between -0.22 and 0.14 (i.e. decimal VA range: 1.80 to 0.72), with the mean being -0.048 ± 0.085 . Institutional research board approval was obtained. The study was conducted in adherence to the tenets of the Declaration of Helsinki and followed a protocol approved by the Institutional Research Board.

2.2 Wavefront sensing

The monochromatic wavefront aberration function of the eye was measured using the Allegretto wavefront analyser (Wavelight Laser Technologies AG, Erlanger, Germany), which is based on the principles of Tscherning aberrometry as described elsewhere [41, 42]. The system uses a 660 nm wavelength laser diode as the light source (with a laser power of 0.2 mW and a total illumination time ~ 40 ms), which passes as an expanded beam through a 13×13 square dot pattern mask (168 dots in total), generating a spot pattern on the retina. According to the manufacturers, the lenslet array samples the exiting wavefront every $210 \mu\text{m}$ in the pupil plane. This allows a maximum of 136 dots within a 7.7 mm pupil diameter (while a 6 mm pupil allows the capture of a 82-dot pattern; see Figure 1). This pattern is captured by a highly sensitive CCD camera linked to a personal computer used for image analysis. Deviations in corresponding spot positions between the ideal and the real pattern are used for the mathematical reconstruction of the wavefront error of the eye. The data extracted from the analyser, consist of a set of Zernike coefficients up to

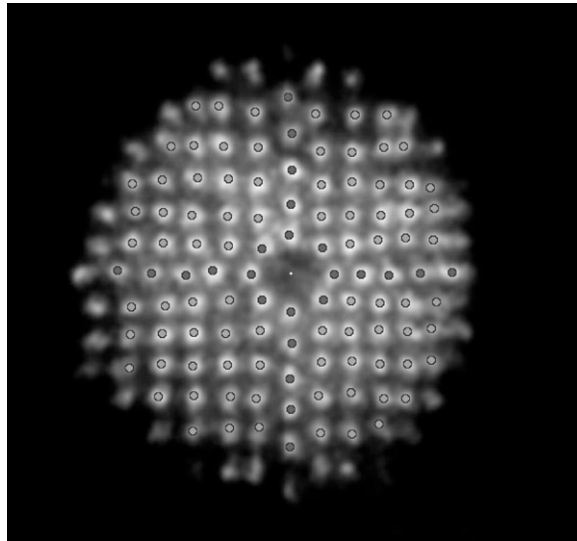


Figure 1. Example of a measured retinal spot pattern for an emmetropic eye. Within a maximum 7.7 mm pupil a 136-spot pattern is captured (a 6 mm pupil allows the capture of an 82-dot pattern). Deviations in corresponding spot positions between the ideal and the real pattern are used for the mathematical reconstruction of the ocular wavefront error.

sixth-order aberrations (27 coefficients in total) in 'Wavelight' format, that quantify the type and the magnitude of aberrations present.

The line-of-sight is determined as the reference axis for the purpose of measuring and calculating aberrations. The alignment and centration of the subject's line-of-sight with the instrument's optical axis is achieved by means of a fixation target (mounted coaxially to the optical axis of the device) and the centre of the pupil. This, as well as pupil diameter, are determined by an infrared LED and the CCD camera that records the reflection of the LED light from the cornea. In addition, the alignment of the z axis is done by centering the iris-reflex of a modified slit lamp onto the pupil centre.

2.3 Procedure

All measurements were carried out with room lights switched off (low mesopic levels) to avoid the need to pharmacologically dilate the pupil. Wavefront aberrations could then be measured over the full extent of a natural pupil (ranged between 6.00 and 8.27 mm). The subject was asked to position his head on the chin rest and look at the centre of the fixation target (black star within a yellow ring). During wavefront sensing, fogging of the fixation target was turned on to allow inhibition of accommodation. The operator manually aligned the subject's pupil centre with the optical axis of the device by means of six dots and a cross-stage. Once the system has detected the pupil, a dotted circle and a window displaying x,y,z offset and pupil diameter data appeared. Subjects were asked to blink 2–3 times, while keeping their eyes wide open prior to the measurement. Four consecutive measurements were taken for each eye: the clearest image was selected for further analysis.

2.4 Data analysis

The files containing wavefront information were downloaded on removable media and processed off-line using programs written in MATLAB (V 5.2, Mathworks, Inc Nantick, MA) mathematical software. The Zernike expansion coefficients derived from the wave inclination data for the full pupil, were initially transposed to the OSA notation (recommended by the Optical Society of America [43]) and corrected for chromatic aberration (from 660 to 550 nm) (see [44]). Piston and tilt coefficients were not included. The corrected coefficients were scaled to a smaller diameter (6 mm) using a matrix method to reconstruct a new set of Zernike coefficients that describe a wavefront aberration corresponding to the central 6 mm of the pupil. To achieve this we used formulas developed by Schwiegerling (see [45]) implemented in a Matlab file, as previously described by Campbell (see [46]). This is important as all available raw data for the full pupil size were used.

3. Results

3.1 Sphero-cylindrical refractive error

Figure 2 presents frequency histograms of the components that define the refractive error of the population tested, i.e. the spherical equivalent (M) and the orthogonal components

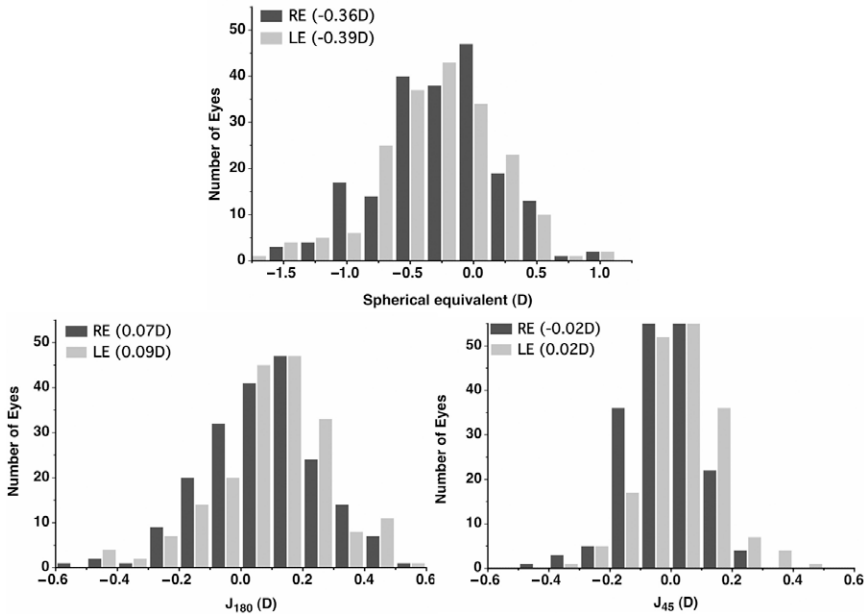


Figure 2. Frequency histograms of Spherical Equivalent (M) (upper panel) and the orthogonal components of astigmatic error (J_{180} and J_{45}) (lower panel) for the right (dark grey bars) and left (light grey bars) eyes. Spherical Equivalent is calculated by the defocus and the spherical aberration terms of Zernike coefficients (see Equation (1)), whereas astigmatic errors are determined by the second-order astigmatic coefficients (c_2^{-2} , c_2^2) (see Equations (2) and (3)). The legend indicates mean values (in D). Number of eyes (N) is: 199 (RE), 194 (LE).

of the astigmatic error (J_{180} and J_{45}). The spherical equivalent was calculated from Equation (1), using ‘paraxial curvature matching’ (i.e. the second-order paraxial focus [c_2^0] and the fourth-order spherical aberration [c_4^0] Zernike coefficients). This forms an approximation of spherical equivalent used in common ophthalmic calculations, which was found to be the most accurate method in predicting subjective refraction [27]. The astigmatic errors were calculated from Equations (2) and (3), using the second-order astigmatic coefficients (c_2^{-2} , c_2^2) and the pupil radius, r , in mm.

$$M = \frac{-c_2^0 4(3^{1/2}) + c_4^0 12(5^{1/2})}{r^2}, \quad (1)$$

$$J_{180} = \frac{-c_2^2 2(6^{1/2})}{r^2}, \quad (2)$$

$$J_{45} = \frac{-c_2^{-2} 2(6^{1/2})}{r^2}. \quad (3)$$

Mean spherical equivalent was found to be -0.36 D for the right eye (RE) (range: -1.84 to $+1.24$ D) and -0.39 D for the left eye (LE) (range: -1.74 to $+1.13$). The values are slightly more myopic when compared to the refractive error measured by the auto-refractometer (RE: -0.26 D, LE: -0.28 D). Moreover, there is a tendency for eyes

Table 1. Average signed Zernike coefficients (in μm) for both eyes of the population tested.

<i>Coefficient</i>	RE($n = 199$)	LE ($n = 194$)
c_2^{-2}	0.043 ± 0.203	-0.058 ± 0.218
c_2^0	0.477 ± 0.583	0.503 ± 0.548
c_2^2	-0.140 ± 0.336	-0.172 ± 0.343
c_3^{-3}	-0.065 ± 0.116	-0.059 ± 0.108
c_3^{-1}	0.011 ± 0.133	-0.006 ± 0.137
c_3^1	-0.011 ± 0.091	0.014 ± 0.100
c_3^3	-0.006 ± 0.091	0.012 ± 0.092
c_4^{-4}	0.014 ± 0.044	-0.010 ± 0.051
c_4^{-2}	-0.003 ± 0.035	0.004 ± 0.038
c_4^0	0.035 ± 0.098	0.038 ± 0.090
c_4^2	0.006 ± 0.053	0.008 ± 0.048
c_4^4	0.013 ± 0.053	0.005 ± 0.049
c_5^{-5}	-0.007 ± 0.024	-0.003 ± 0.024
c_5^{-3}	0.005 ± 0.018	0.000 ± 0.019
c_5^{-1}	-0.007 ± 0.024	-0.003 ± 0.019
c_5^1	0.000 ± 0.019	0.000 ± 0.020
c_5^3	0.002 ± 0.018	0.000 ± 0.017
c_5^5	0.002 ± 0.026	-0.003 ± 0.028
c_6^{-6}	-0.002 ± 0.018	0.001 ± 0.017
c_6^{-4}	0.001 ± 0.012	-0.002 ± 0.013
c_6^{-2}	0.000 ± 0.010	-0.001 ± 0.011
c_6^0	-0.003 ± 0.020	-0.004 ± 0.018
c_6^2	0.000 ± 0.013	-0.002 ± 0.013
c_6^4	0.001 ± 0.013	0.003 ± 0.012
c_6^6	0.000 ± 0.013	-0.002 ± 0.012

showing ‘with-the-rule’ astigmatism, since mean J_{180} is positive (RE: 0.07, LE: 0.09) (Figure 2).

3.2 Distribution of wavefront aberrations

The mean signed value (± 1 SD) of each Zernike coefficient (up to sixth order) for right and left eyes is depicted in Table 1. The same information is illustrated in a pyramid structure in Figure 3. For the interpretation of the magnitude of each mode, the equivalent defocus error (M_e) of each coefficient is also shown. This is defined as the amount of defocus required to produce the same root-mean-squared [RMS] wavefront error, by one or more higher-order modes (see Equation (4)).

$$M_e = 4(3^{1/2}) \frac{\text{RMS error}}{r^2}. \quad (4)$$

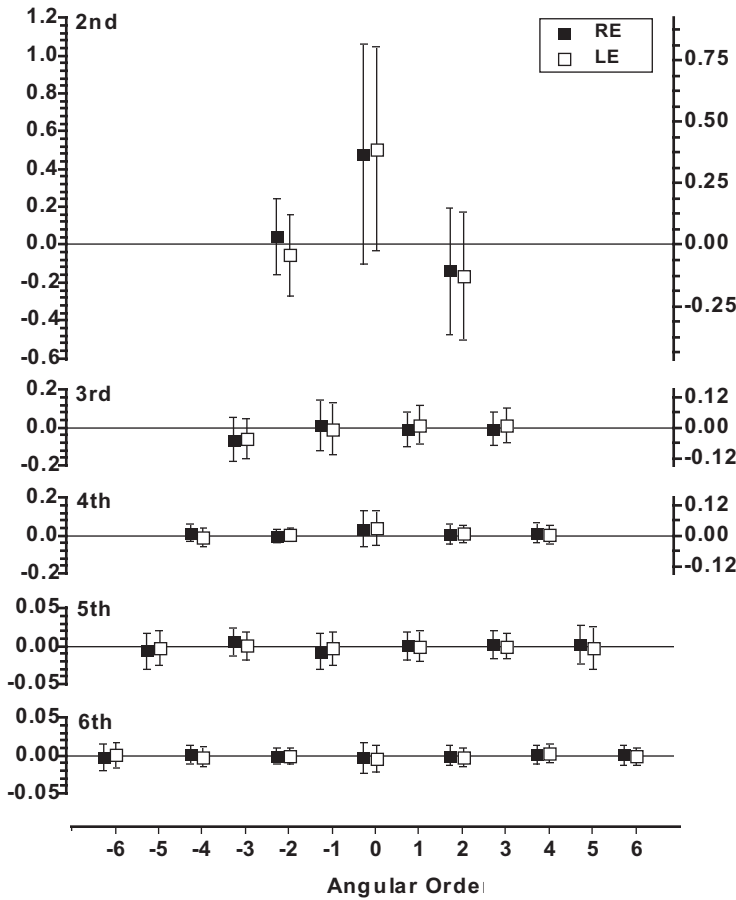


Figure 3. Mean values (± 1 SD) of all Zernike coefficients for right (filled squares) and left (empty squares) eyes displayed in the characteristic pyramidal format. The scale on the right refers to the equivalent defocus of each term (see Equation (4)). 6 mm pupils are used for analysis. Number of eyes (N) is: 199 (RE), 194 (LE).

Although second-order aberrations, i.e. myopic defocus (c_2^0) and cartesian astigmatism (c_2^2), are by far the most dominant, the greatest relative inter-subject variability (when weighted by its absolute value) is observed for the higher order aberrations. It is also evident that the population averages of Zernike coefficients are almost zero except primary spherical aberration (c_4^0) and oblique trefoil (c_3^{-3}).

Frequency histograms of the RMS wavefront error of higher order (third to sixth order) coefficients are depicted in Figure 4. Mean RMS values are $0.26 \mu\text{m}$ (range: 0.11 to $0.54 \mu\text{m}$) for right eyes and $0.26 \mu\text{m}$ (range: 0.11 to $0.61 \mu\text{m}$) for left eyes, which corresponds to an average equivalent defocus (M_e) of 0.20 D (range: 0.09 to 0.47 D) and 0.20 D (range: 0.09 to 0.42 D), respectively. The distribution of higher-order RMS, as indicated by the Shapiro–Wilk test, is not normal.

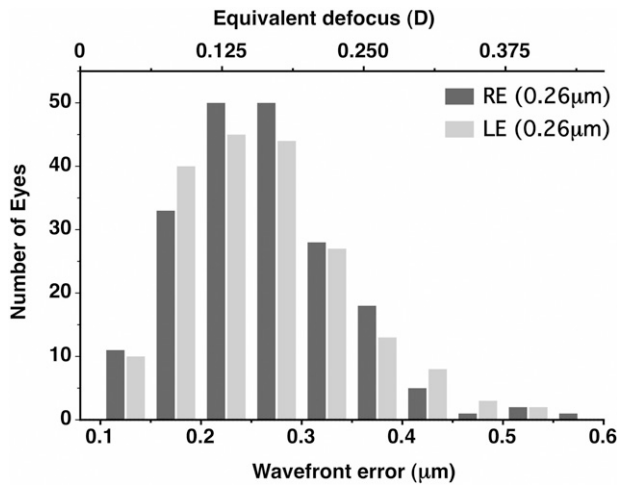


Figure 4. Frequency histograms of the higher-order wavefront RMS error from right (dark grey bars) and left (light grey bars) eyes. The scale on the top refers to the equivalent defocus. The legend indicates mean values (in μm). Pupil diameter is 6 mm. Number of eyes (N) is: 199 (RE), 194 (LE).

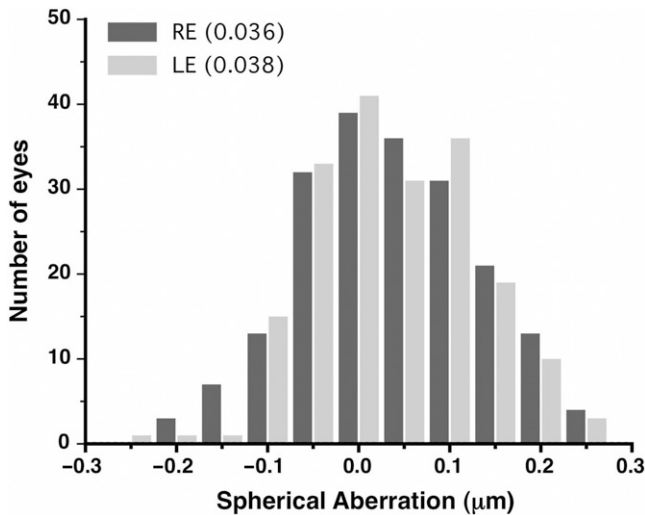


Figure 5. Frequency histograms of spherical aberration from right (dark grey bars) and left (light grey bars) eyes. The legend indicates mean values (in μm). Pupil diameter is 6 mm. Number of eyes (N) is: 199 (RE), 194 (LE).

Figure 5 illustrates frequency histograms of the fourth-order spherical aberration. Mean spherical aberration is $0.035\mu\text{m}$ (range: -0.22 to $0.26\mu\text{m}$) for right eyes and $0.038\mu\text{m}$ (range: -0.23 to $0.30\mu\text{m}$) for left eyes. Shapiro–Wilk testing showed that the distribution of spherical aberration is not normal.

Table 2. Correlation coefficients for each Zernike mode between right and left eyes. The asterisk indicates the modes that are significantly correlated ($p < 0.05$).

c_2^{-2}	c_2^0	c_2^2					
-0.39*	0.58*	0.71*					
c_3^{-3}	c_3^{-1}	c_3^1	c_3^3				
0.54*	0.74*	-0.46*	-0.30*				
c_4^{-4}	c_4^{-2}	c_4^0	c_4^2	c_4^4			
0.03	-0.13	0.82*	0.42*	0.25			
c_5^{-5}	c_5^{-3}	c_5^{-1}	c_5^1	c_5^3	c_5^5		
0.17	0.26	0.41*	0.29*	-0.01	-0.15		
c_6^{-6}	c_6^{-4}	c_6^{-2}	c_6^0	c_6^2	c_6^4	c_6^6	
0.03	0.07	0.04	0.61*	-0.06	0.16	0.13	

3.3 Bilateral symmetry

Table 2 shows correlation coefficients for each Zernike term between left and right eyes. Primary spherical aberration (c_4^0) had the highest correlation coefficient (0.82), followed by vertical coma (c_3^{-1} , 0.74), 90/180 (cartesian) astigmatism (c_2^2 , 0.71), secondary spherical aberration (c_6^0 , 0.62) and defocus (c_2^0 , 0.58). Figure 6 plots the correlation of zero angular orders and the even- and odd-symmetric higher-order aberrations between the two eyes. The correlation coefficient, r , is higher for the zero angular orders (0.72), followed by the even-symmetric (0.67) and the odd-symmetric terms (0.38). Correlations between eyes are significant ($p < 0.05$) for all the second- and third-order terms.

3.4 Ageing

The effect of ageing on RMS wavefront error for higher-order (third to sixth order) and coma-like aberrations (c_3^{-1} , c_3^1 , c_5^{-1} , c_5^1) is shown in Figure 7. Although a substantial inter-subject variability is evident, which results in non-statistically significant correlations ($p=0.22$ and $p=0.23$, correspondingly), there is a tendency for both combined higher-order and coma-like aberration to increase with age. Conversely, no systematic change is observed for spherical aberration (Figure 7(b)). Moreover, Figure 7(a) shows that ageing is accompanied by pupillary miosis. It appears that pupil diameter decreases with age, with a rate of about 0.25 mm per decade.

4. Discussion

The current study investigated wavefront aberration statistics in an emmetropic adult population. The distribution patterns of individual modes agree with previous studies, showing a significant dispersion in all Zernike coefficients among normal eyes. Second-order (sphero-cylindrical) terms dominate, while the mean of most of the higher-order coefficients is close to zero. The most prominent higher-order aberrations for a 6 mm pupil are oblique trefoil (c_3^{-3} , -0.062) and primary spherical aberration (c_4^0 , 0.037). The latter is found to be non-zero and positive in sign in all large population studies (see Salmon and van de Pol [47] for a review). However, its magnitude (mean signed

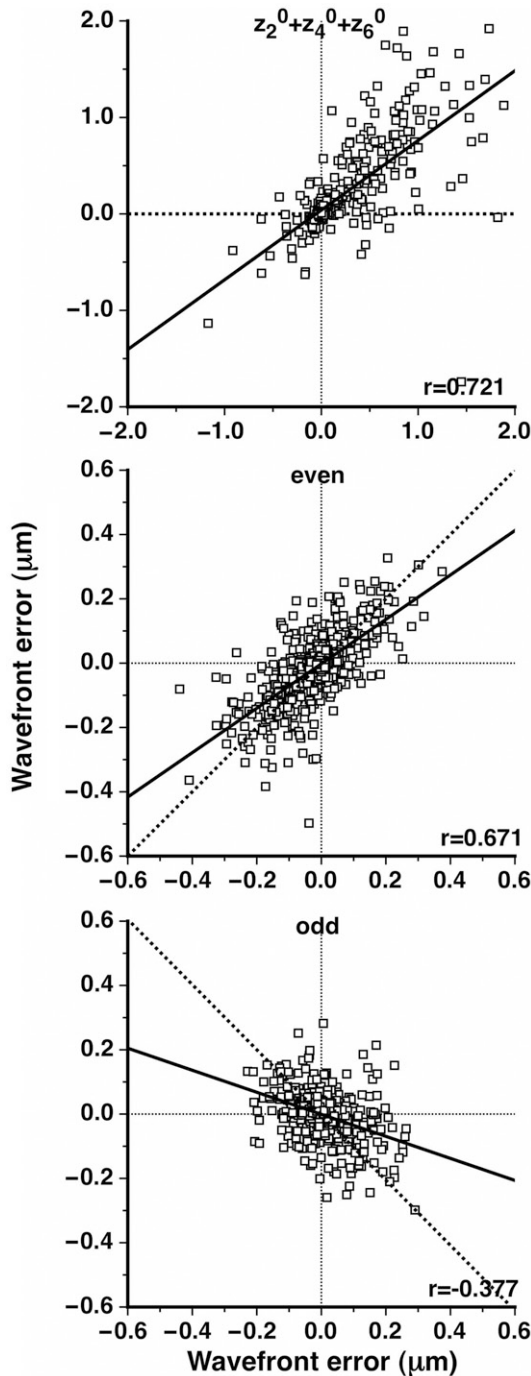


Figure 6. Correlation of zero angular orders (c_2^0 , c_4^0 , c_6^0 – top) as well as even (middle) and odd (bottom) symmetric higher-order aberrations between the two eyes. The solid lines represent least-squares regression fits, whereas the dotted lines the one-to-one predictions. The legend indicates the correlation coefficient, r .

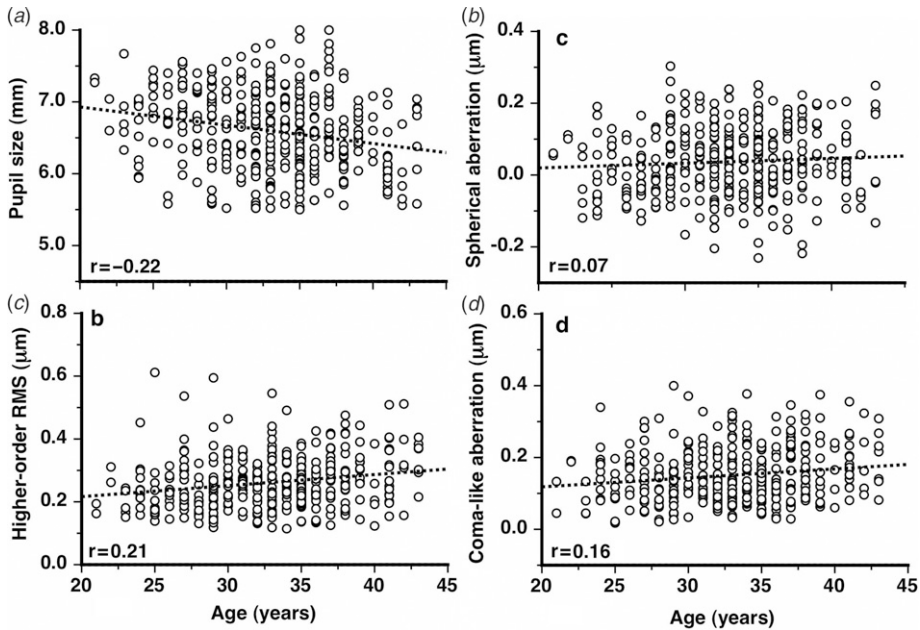


Figure 7. Plots of (a) pupil size and RMS wavefront error for (b) higher-order, (c) spherical and (d) coma-like aberrations as a function of the age of the population tested. Data from both eyes are included ($N=396$). 6mm pupils are used for wavefront error analysis. The dashed lines represent least-squares regression fits. The legend indicates the correlation coefficient, r .

value: $0.036\ \mu\text{m}$ for RE and $0.038\ \mu\text{m}$ for LE; mean absolute value: $0.083\ \mu\text{m}$ for RE and $0.078\ \mu\text{m}$ for LE) is significantly lower than reported in previous studies [4–7, 48]. Since there is evidence that the Allegreto wavefront analyser produces similar spherical aberration values with other commercially available clinical aberrometers [49], the lower signed and absolute mean values are possibly due to the high percentage of eyes found with negative spherical aberration (37% of right and 35% of left eyes), which corresponds to over-corrected spherical aberration. Furthermore, the mean signed values of both vertical and horizontal coma have mean values close to zero, converse to previous studies which usually show significant non-zero mean coefficients for all third-order aberrations. As a result of the lower magnitudes of individual Zernike modes, mean higher-order RMS is of smaller magnitude ($0.26\ \mu\text{m}$ in both eyes), compared to $0.33\ \mu\text{m}$, which is the expected mean value in the normal adult eye [47]. Another interesting observation is that some eyes show exceptionally good retinal quality, in the absence of any sphero-cylindrical error, with higher-order RMS being less than $0.15\ \mu\text{m}$.

Although, several authors have found higher levels of individual (e.g. spherical aberration, and vertical coma) and combined aberrations in myopes as compared to emmetropes [38, 39], there is actually little evidence for systematically larger higher-order aberrations in myopia [50]. Conversely, other studies [36, 51] reported that adult myopes show less positive spherical aberration than emmetropes. The conflicting conclusions between individual studies may be explained by differences in subject groups, i.e. ages and

racial backgrounds, and the measuring or analysis methods. The results of the current study cannot be directly correlated with the majority of large-scale studies, which have used trial lenses to correct spherocylindrical error [7, 13, 35, 52]. There is a possibility that, in the previous studies, the magnitude of higher-order aberrations might have been overestimated, due to a failure to correct for the pupil magnification caused by the use of spectacle correction. Atchison and Charman [40] pointed out that, in the case a 6 D myopia is corrected with spectacle lenses placed at 12 mm in front of the eye, pupil magnification results in a 50% increase in spherical aberration.

Nevertheless, this work suggests that a large number of individuals with low refractive error, show modest amounts of Zernike coefficients and combined wavefront errors, significantly lower to the values reported on myopic eyes by previous studies. The increased spherical aberration in myopia may be expected in view of changes in corneal asphericity, i.e. the reduced peripheral flattening of cornea observed in myopic eyes [53, 54], although more recent studies [55] found no significant effect of refraction on asphericity. It is obvious, that in order to reach safe conclusions, regarding the role of higher-order aberrations and their corresponding retinal blur in myopia development, longitudinal studies should be addressed.

In addition, the present work demonstrates a considerable tendency for the aberrations to be symmetric between left and right eyes, confirming earlier studies [6, 7, 52]. The highest bilateral symmetry is observed for the zero angular orders (primary and secondary spherical aberration), while the correlation coefficient for myopic defocus is low, when compared to other studies, possibly due to the small magnitude of defocus in the emmetropic group.

Regarding the effect of ageing on aberrations, it appears that, for a fixed pupil diameter (6 mm), combined aberration levels increase with age through adulthood. This increase seems to be mainly due to changes in coma-like aberrations, attributed to corneal changes, as also pointed out by previous research [4, 14, 15, 56]. However, for the specific age-range of the group tested (21 to 43 years) no change in spherical aberration was observed. This is in agreement with other reports [13, 15, 17], which found that spherical aberration does not change until about the fourth decade, after which it increases. This hints that either pre-presbyopic changes in the lens shape and size do not affect spherical aberration [15], or they are compensated by concurrent changes in corneal asphericity [4]. However, it should be emphasised, that some compensation in retinal image degradation produced by aberrations is provided by pupil sizes decreasing with age [57–59]. This study highlights a 0.25 mm rate of decrease of pupil size per decade under low mesopic levels (see Figure 7(b)) close to previously reported values [59]. It is expected that senile miosis would maintain retinal image quality at an approximately constant level, with visual degradation mainly arising from intraocular scattered light [31, 34].

Acknowledgements

The authors acknowledge Ioannis Aslanides, Sophia Panagopoulou, Dimitris Tsatsaronis and Nikolaos Astyrakakis for their help in data acquisition. Preliminary results of this study were presented at the Association for Research in Vision and Ophthalmology, Ft. Lauderdale, FL, in April 2004.

References

- [1] Koomen, M.J.; Scolnik, R.; Tousey, R. *J. Opt. Soc. Am.* **1956**, *46*, 903–904.
- [2] Jenkins, T.C.A. *Br. J. Physiol. Opt.* **1963**, *20*, 59–91.
- [3] Smirnov, M.S. *Biofizika* **1961**, *6*, 776–795.
- [4] Amano, S.; Amano, Y.; Yamagami, S.; Miyai, T.; Miyata, K.; Samejima, T.; Oshika, T. *Am. J. Ophthalmol.* **2004**, *137*, 988–992.
- [5] Castejon-Mochon, J.F.; Lopez-Gil, N.; Benito, A.; Artal, P. *Vision Res.* **2002**, *42*, 1611–1617.
- [6] Porter, J.; Guirao, A.; Cox, I.G. et al. *J. Opt. Soc. Am. A Opt. Image Sci. Vis.* **2001**, *18*, 1793–1803.
- [7] Thibos, L.N.; Hong, X.; Bradley, A.; Cheng, X. *J. Opt. Soc. Am. A Opt. Image Sci. Vis.* **2002**, *19*, 2329–2348.
- [8] Wang, Y.; Zhao, K.X.; Jin, Y.; Niu, Y.F.; Zuo, T. *J. Refract. Surg.* **2003**, *19*, S270–S274.
- [9] Applegate, R.A. *Optom. Vis. Sci.* **2004**, *81*, 167–177.
- [10] Marsack, J.D.; Thibos, L.N.; Applegate, R.A. *J. Vis.* **2004**, *4*, 322–328.
- [11] Atchison, D.A.; Collins, M.J.; Wildsoet, C.F.; Christensen, J.; Waterworth, M.D. *Vis. Res.* **1995**, *35*, 313–323.
- [12] Yoon, G.Y.; Williams, D.R. *J. Opt. Soc. Am. A Opt. Image Sci. Vis.* **2002**, *19*, 266–275.
- [13] Brunette, I.; Bueno, J.M.; Parent, M.; Hamam, H.; Simonet, P. *Invest. Ophthalmol. Vis. Sci.* **2003**, *44*, 5438–5446.
- [14] Guirao, A.; Redondo, M.; Artal, P. *J. Opt. Soc. Am. A Opt. Image Sci. Vis.* **2000**, *17*, 1697–1702.
- [15] Wang, L.; Santaella, R.M.; Booth, M.; Koch, D.D. *J. Cataract Refract. Surg.* **2005**, *31*, 1512–1519.
- [16] Buehren, T.; Collins, M.J.; Carney, L.G. *Vis. Res.* **2005**, *45*, 1297–1312.
- [17] He, J.C.; Burns, E.; Marcos, S.A. *Vision Res.* **2000**, *40*, 41–48.
- [18] Plainis, S.; Ginis, H.S.; Pallikaris, A. *J. Vis.* **2005**, *5*, 466–477.
- [19] Chalista, M.R.; Krueger, R.R. *Ophthalmol. Clin. North Am.* **2004**, *17*, 135–142, v–vi.
- [20] Llorente, L.; Barbero, S.; Merayo, J.; Marcos, S. *J. Refract. Surg.* **2004**, *20*, 203–216.
- [21] Marcos, S.; Barbero, S.; Llorente, L.; Merayo-Lloves, J. *Invest. Ophthalmol. Vis. Sci.* **2001**, *42*, 3349–3356.
- [22] Seiler, T.; Kaemmerer, M.; Mierdel, P.; Krinke, H.E. *Arch. Ophthalmol.* **2000**, *118*, 17–21.
- [23] Yamane, N.; Miyata, K.; Samejima, T.; Hiraoka, T.; Kiuchi, T.; Okamoto, F.; Hirohara, Y.; Mihashi, T.; Oshika, T. *Invest. Ophthalmol. Vis. Sci.* **2004**, *45*, 3986–3990.
- [24] Yoon, G.; Macrae, S.; Williams, D.R.; Cox, I.G. *J. Cataract Refract. Surg.* **2005**, *31*, 127–135.
- [25] Cheng, X.; Bradley, A.; Thibos, L.N. *J. Vis.* **2004**, *4*, 310–321.
- [26] Salmon, T.O.; West, R.W.; Gasser, W.; Kenmore, T. *Optom. Vis. Sci.* **2003**, *80*, 6–14.
- [27] Thibos, L.N.; Hong, X.; Bradley, A.; Applegate, R.A. *J. Vis.* **2004**, *4*, 329–351.
- [28] Campbell, F.W.; Gubisch, R.W. *J. Physiol. (London)* **1966**, *186*, 558–578.
- [29] Walsh, G.; Charman, W.N.; Howland, H.C. *J. Opt. Soc. Am. A Opt. Image Sci. Vis.* **1984**, *1*, 987–992.
- [30] Charman, W.N.; Chateau, N. *Ophthalm. Physiol. Opt.* **2003**, *23*, 479–493.
- [31] Ijspeert, J.; de Waard, P.W.; van den Berg, T.J.; de Jong, P.T. *Vis. Res.* **1990**, *30*, 699–707.
- [32] Kuroda, T.; Fujikado, T.; Ninomiya, S.; Maeda, N.; Hirohara, Y.; Mihashi, T. *J. Refract. Surg.* **2002**, *18*, S598–S602.
- [33] Shahidi, M.; Yang, Y. *Optom. Vis. Sci.* **2004**, *81*, 853–857.
- [34] van den Berg, T.J. *Optom. Vis. Sci.* **1995**, *72*, 52–59.
- [35] Campbell, F.W.; Gubisch, R.W. *J. Physiol. (London)* **1967**, *192*, 345–358.
- [36] Carkeet, A.; Luo, H.D.; Tong, L.; Saw, S.M.; Tan, D.T.H. *Vis. Res.* **2002**, *42*, 1809–1824.
- [37] Cheng, X.; Bradley, A.; Hong, X.; Thibos, L.N. *Optom. Vis. Sci.* **2003**, *80*, 43–49.
- [38] He, J.C.; Sun, P.; Held, R.; Thom, F.; Sun, X.R.; Gwiazda, J.E. *Vis. Res.* **2002**, *42*, 1063–1070.
- [39] Paquin, M.P.; Hamam, H.; Simonet, P. *Optom. Vis. Sci.* **2002**, *79*, 285–291.
- [40] Atchison, D.A.; Charman, W.N. *J. Opt. Soc. Am. A Opt. Image Sci. Vis.* **2005**, *22*, 2589–2597.
- [41] Krueger, R.R.; Mrochen, M.; Kaemmerer, M.; Seiler, T. *Ophthalmology* **2001**, *108*, 674–678.

- [42] Rozema, J.J.; Van Dyck, D.E.; Tassignon, M.J. *J. Cataract Refract. Surg.* **2005**, *31*, 1114–1127.
- [43] Thibos, L.N.; Applegate, R.A.; Schwiegerling, J.T.; Webb, R. *J. Refract. Surg.* **2000**, *16*, S654–S655.
- [44] Ginis, H.S.; Plainis, S.; Pallikaris, A. *BMC Ophthalmol.* **2004**, *4*, 1.
- [45] Schwiegerling, J. *J. Opt. Soc. Am. A Opt. Image Sci. Vis.* **2002**, *19*, 1937–1945.
- [46] Campbell, C.E. *J. Opt. Soc. Am. A Opt. Image Sci. Vis.* **2003**, *20*, 209–217.
- [47] Salmon, T.O.; van de Pol, C. *J. Cataract Refract. Surg.* **2006**, *32*, 2064–2074.
- [48] Wang, L.; Koch, D.D. *J. Cataract Refract. Surg.* **2003**, *29*, 1896–1903.
- [49] Rozema, J.J.; Van Dyck, D.E.; Tassignon, M.J. *J. Cataract Refract. Surg.* **2006**, *32*, 33–44.
- [50] Charman, W.N. *Ophthalm. Physiol. Opt.* **2005**, *25*, 285–301.
- [51] Collins, M.J.; Wildsoet, C.F.; Atchison, D.A. *Vis. Res.* **1995**, *35*, 1157–1163.
- [52] Wang, L.; Dai, E.; Koch, D.D.; Nathoo, A. *J. Cataract Refract. Surg.* **2003**, *29*, 1514–1521.
- [53] Carney, L.G.; Mainstone, J.C.; Henderson, B.A. *Invest. Ophthalmol. Vis. Sci.* **1997**, *38*, 311–320.
- [54] Horner, D.G.; Soni, P.S.; Vyas, N.; Himebaugh, N.L. *Optom. Vis. Sci.* **2000**, *77*, 198–203.
- [55] Atchison, D.A. *Vis. Res.* **2006**, *46*, 2236–2250.
- [56] Oshika, T.; Klyce, S.D.; Applegate, R.A.; Howland, H.C. *Invest. Ophthalmol. Vis. Sci.* **1999**, *40*, 1351–1355.
- [57] Calver, R.I.; Cox, M.J.; Elliott, D.B. *J. Opt. Soc. Am. A Opt. Image Sci. Vis.* **1999**, *16*, 2069–2078.
- [58] Charman, W.N. *Optom. Vis. Sci.* **2006**, *83*, 335–345.
- [59] Winn, B.; Whitaker, D.; Elliott, D.B.; Phillips, N.J. *Invest. Ophthalmol. Vis. Sci.* **1994**, *35*, 1132–1137.